



G030

Seismic Data Reconstruction Using Multidimensional Prediction Filters

M. Naghizadeh* (University of Alberta) & M.D. Sacchi (University of Alberta)

SUMMARY

The Multi-Step Auto-Regressive (MSAR) reconstruction method is extended to reconstruct multidimensional seismic data. The validity of MSAR prediction filtering estimation for more than one spatial coordinate is proved. In addition, simple graphical interpretations are provided in order to explain the details pertaining the practical implementation of our algorithm. Finally, the performance of MSAR on synthetic 2D and 3D data set and a real 3D data example are examined.

Introduction

Auto-Regressive (AR) modeling has a broad range of applications in signal processing. An auto-regressive operator utilizes the time history of a signal to extract important information hidden in the signal. It has been widely utilized in the area of spectrum estimation, as well as signal filtering.

One of the main applications of AR modeling is signal prediction. Spitz (1991) and Porsani (1999) used AR modeling to interpolate the regularly sampled seismic records in the spatial direction. Also, Naghizadeh and Sacchi (2007a) introduced the Multi-Step Auto-Regressive (MSAR) algorithm in order to reconstruct nonuniformly sampled data in the spatial direction. The latter is a novel way of applying AR operation with jumping steps in the low frequency portion of the data in an attempt to extract AR operators for the high frequency portion. The extracted Prediction Filter (PF) for each frequency is then used as a regularization term to reconstruct the missing spatial samples.

In this paper we investigate the performance of MSAR algorithm for more than one spatial direction. First, in the theory section, an optimality proof of multidimensional (MD) MSAR algorithm is discussed. Then a practical implementation of MSAR using simple flowcharts is discussed. Finally, synthetic and real data examples of application of MSAR are shown.

Theory

For simplicity we consider the example with two spatial coordinates. Generalization to more than two spatial coordinates is straightforward. Consider a 3D cube composed of dipping planes. Each plane can be characterized by its slope p_k with components on each spatial axis i.e. p_{x_k} and p_{y_k} . A 2D array signal in p_{x_k} the frequency-space-space domain can be represented as:

$$G(l\Delta x, m\Delta y, n\Delta f) = \sum_{k=1}^K A_k(n\Delta f) \cdot \exp[-i2\pi(n\Delta f) \cdot \sqrt{(l\Delta x \cdot p_{x_k})^2 + (m\Delta y \cdot p_{y_k})^2}], \quad (1)$$

where, $A_k(n\Delta f)$ is the amplitude of each event at the frequency $n\Delta f$. The root square term represents the amount of time-shift for the specific receiver in comparison to the reference receiver. The distance between receivers is proportional to the amount of time shift due to the linearity of the events. Now consider the case $\Delta x' = \alpha\Delta x$, $\Delta y' = \alpha\Delta y$ and $\Delta f' = \Delta f / \alpha$. It can be easily proven that:

$$G(l\Delta x, m\Delta y, n\Delta f) = G(l\Delta x', m\Delta y', n\Delta f') \quad (2)$$

Since the signal G consists of superposition of harmonics, it can be well represented by a set of 2D AR operators as below:

$$G(l\Delta x, m\Delta y, n\Delta f) = \sum_{r=0}^R \sum_{\substack{s=0 \text{ if } r \neq 0 \\ s=1 \text{ if } r=0}}^S P(r, s, n\Delta f) \cdot G((l-r)\Delta x, (m-s)\Delta y, n\Delta f), \quad (3)$$

where, P is the desired AR operator with the orders R and S in x and y directions, respectively. Writing the same AR equations for $\Delta x'$, $\Delta y'$ and $\Delta f'$, we have:

$$G(l\Delta x', m\Delta y', n\Delta f') = \sum_{r=0}^R \sum_{\substack{s=0 \text{ if } r \neq 0 \\ s=1 \text{ if } r=0}}^S P'(r, s, n\frac{\Delta f}{\alpha}) \cdot G((l-r)\alpha\Delta x, (m-s)\alpha\Delta y, n\frac{\Delta f}{\alpha}) \quad (4)$$

It can be easily concluded from equations (2), (3) and (4) that:

$$P'(r, s, n\frac{\Delta f}{\alpha}) = P(r, s, n\Delta f) \quad (5)$$

The interpretation of equation (5) is that the multidimensional AR operators computed at frequency $f' = \frac{f}{\alpha}$ by decimating data in all spatial directions by factor of α , are equal to the AR operators that one can compute at frequency f using ordinary multidimensional AR

operators. We name this unique way of applying AR operation as Multi-Step AR (MSAR) operator. The order of 2D AR operator depends on the apparent slope of events in each spatial direction. For a 2D array of receivers with size equal to $L \times M$ and 2D AR operator with the order $R \times S$, the maximum number of jumping steps is obtained by:

$$\alpha_{\max} = \min \left\{ \left\lfloor \frac{L - \frac{R+1}{2}}{R} \right\rfloor, \left\lfloor \frac{M - \frac{S+1}{2}}{S} \right\rfloor \right\} \quad (6)$$

Generalization of the 2D spatial case for more spatial dimensions is straightforward. For the MD spatial coordinates one needs to use MD AR operators in the same fashion as the one discussed for the 2D case.

Practical implementation

The first step of the MSAR method is to use Minimum Weighted Norm Interpolation (MWNI) method with proper band-limiting operators for each chosen frequency in order to reconstruct the low frequency data. This consists of an iterative least square optimization routine using successive FFT transforms. Interested readers can find the details of the MWNI in Liu and Sacchi (2004).

Once we have regularly sampled data, we can use AR operation to find PFs for all the frequencies using only the low frequencies. Figure 1a shows a simple example of computing PFs for different jumping steps as well as its limitations. PFs are computed by making a linear system of equations using forward and backward prediction for each jumping step. For this specific example, with 20 data samples and length of PFs equal to 3, the number of resulting equations for a linear system is shown in the yellow squares at the right hand side of the Figure 1a for different jumping steps. For this example, the maximum jumping step α_{\max} is 6. it should be mentioned that the backward prediction is applied on the complex conjugate of the data samples. Figure 1b is a schematic representation of the extension of 1D PFs to 2D PFs.

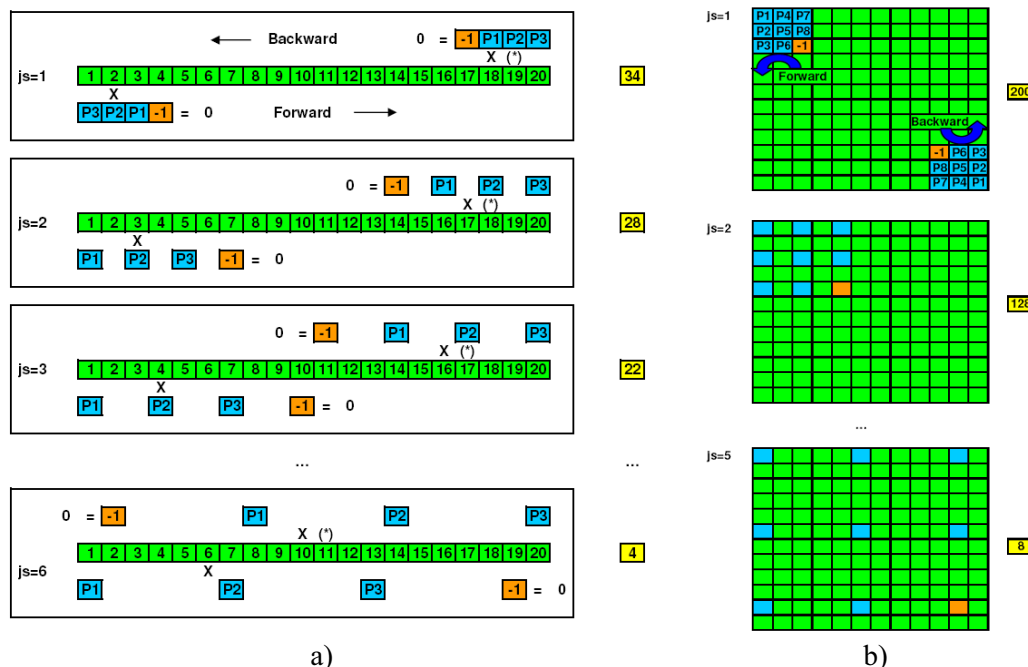


Figure1: Estimation of prediction filters using MSAR for a) 1D case and b) 2D case.

Figure 2 summarizes all the operations for the 1D case. Figure 2a shows how to find PFs from a time series. From the available 10 samples of data indicated by green cells we try to find a PF, shown by blue cells. The linear system of equations in the bottom shows the system

that has to be solved to find the prediction filter. Notice that for simplicity of representation we just show the forward prediction. Predicting missing samples using PFs is the final step of the MSAR method. Once the values of the prediction filters are known one can use them to find the values of missing samples in the signal. Figure 2b shows how to make a linear system of equations in order to find the missing samples (red cells) from known samples (green cells), utilizing a known PF. We separate the columns of the resulted matrix to the green cells (multiplied on known samples) and the red cells (multiplied by unknown samples). The final step, shown in Figure 2c, is to move known samples with their correspondent columns of the matrix to the right hand side and leave the unknowns on the left hand side. This way we obtain a system of equations that can be solved to find the unknown samples.

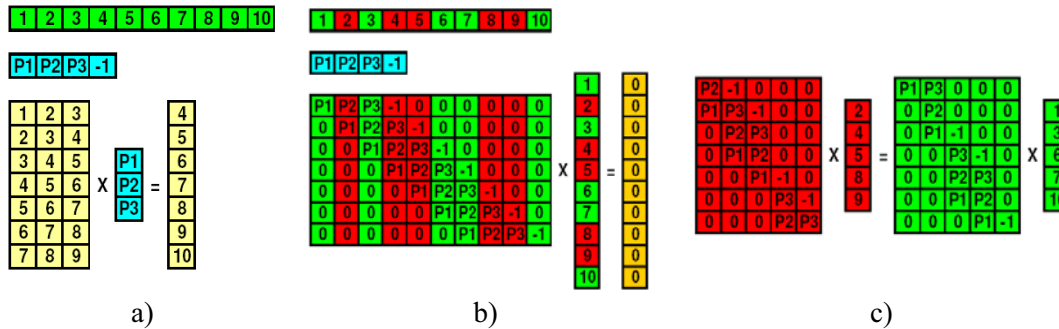


Figure 2: a) Estimating PFs from data; b,c) Estimating unknown data samples using PFs.

Examples

The first example is a 3D synthetic data set composed of three dipping planes which are aliased in both spatial directions. Figure 3a shows slice representation of original data. By replacing every other section in the Y direction with zero sections, we made a cube of data with missing traces shown in Figure 3b. First we reconstruct the low frequency portion of the data using MWN which is shown in Figure 3c. Next, 2D PFs are extracted from the reconstructed low frequency portion for all the frequencies using MSAR algorithm. The missing samples are reconstructed using PFs for all frequencies and result of reconstruction is shown in Figure 3d.

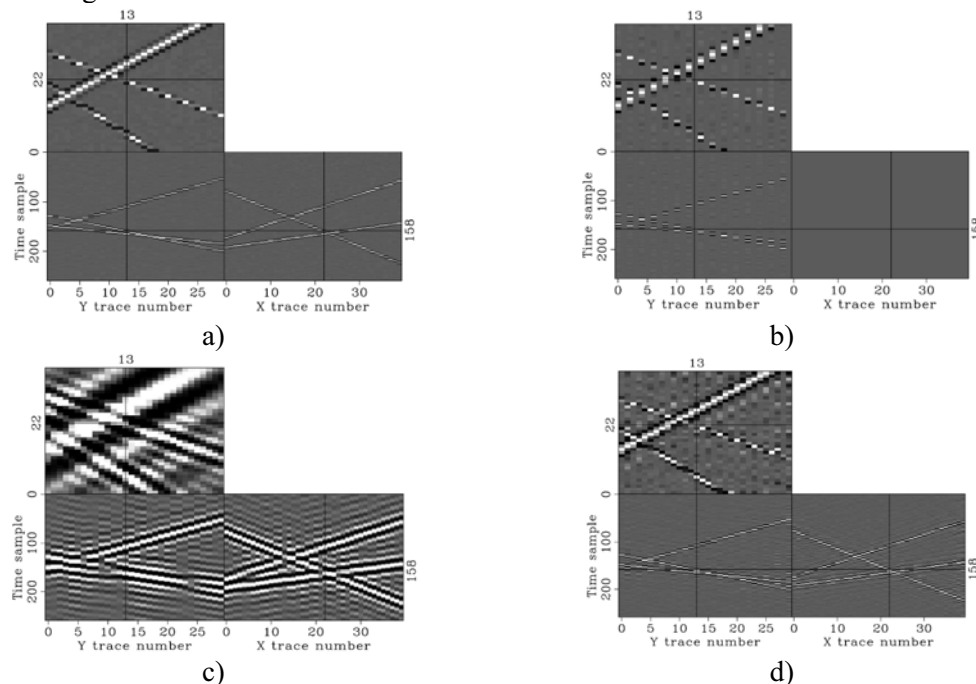


Figure 3: Synthetic 3D example. a) Original data; b) Data with missing sections; c) Reconstructed low frequency data using MWNI; d) Reconstructed data using MSAR.

For the next example, we chose a real data set from Gulf of Mexico. We picked 19 consecutive shots each with 91 traces, each trace with 900 time samples. Later, we eliminated every other shot to make a cube of data with missing traces. A window of data from shots 7 to 11 and from time 3.0 s to 4.0 s is chosen for illustration purposes. Figures 4a and 4b show the windowed original and missing data, respectively. The low frequency part of the data is reconstructed using MWNI and it is shown in Figure 4c. Later, utilizing the MSAR routine, 5×3 size 2D PFs are extracted for all frequencies. Finally, the missing traces were reconstructed using 2D AR modeling. Figure 4d shows the result of reconstruction using 2D PFs. It is clear that 2D PFs were able to utilize the low frequency information to reconstruct the high frequencies.

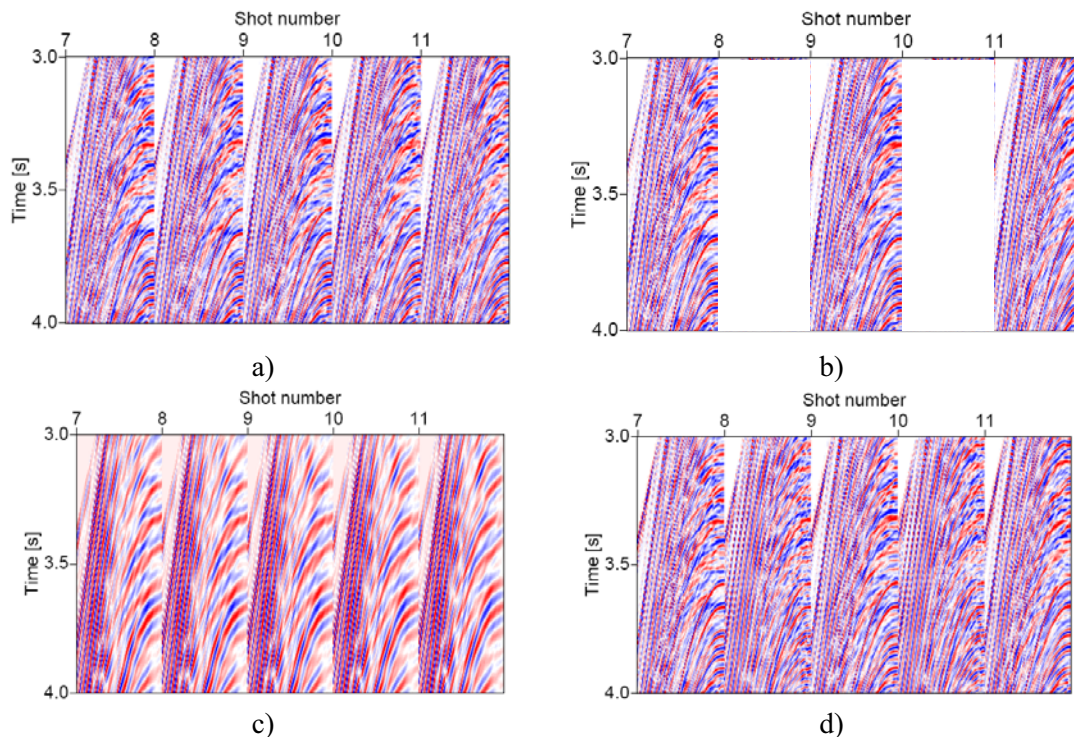


Figure 4: 3D real data example. a) Original data; b) Missing data; c) Reconstructed low frequency data using MWNI; d) Reconstructed data using MSAR

Conclusion

In this paper, the MSAR reconstruction method is extended for multidimensional data. The results of 2D and 3D synthetic data reconstruction, and also the real 3D data example, show that MSAR is capable of reconstructing multidimensional data. Extracting PFs from different low frequencies for a specific high frequency and utilizing their average as an optimal PF for reconstructing missing spatial also helps in reducing estimation errors. The latter is important because one or more single monochromatic low frequencies could be severely contaminated by noise. This is particularly true when processing land data.

References

- Liu, B. and M. D. Sacchi [2004] Minimum weighted norm interpolation of seismic records. *Geophysics*, 69 (6), 1560–1568.
- Naghizadeh, M. and M. D. Sacchi [2007] Multi-step auto-regressive reconstruction of seismic records. *Geophysics*, 72 (6), V111–V118.
- Spitz, S. [1991] Seismic trace interpolation in the F-X domain. *Geophysics*, 56 (6), 785–796.
- Porsani, M. [1999] Seismic trace interpolation using half-step prediction filters. *Geophysics*, 64 (5), 1461–1467.